Available online at www.sciencedirect.com

SciVerse ScienceDirect

journal homepage: www.elsevier.com/locate/he

Time-resolved *in situ* XANES study of the redox properties of $Ce_{0.9}Zr_{0.1}O_2$ mixed oxides

M.G. Zimicz [a,*], S.A. Larrondo [a,b], R.J. Prado [c], D.G. Lamas [d]

[a] Centro de Investigaciones en Sólidos CINSO-CONICET-CITEDEF, J.B. de La Salle 4397, (B1603ALO) Villa Martelli, Pcia. Buenos Aires, Argentina

[b] Laboratorio de Procesos Catalíticos, Depto. de Ing. Química, FIUBA Buenos Aires, Pab. Industrias, Ciudad Universitaria, (C1428EGA) Ciudad Autónoma de Buenos Aires, Argentina

[c] Instituto de Física, Universidade Federal de Mato Grosso, Av. Fernando Corrêa s/n, 78060-900, Cuiabá, MT, Brazil

[d] Laboratorio de Caracterización de Materiales, Facultad de Ingeniería, Universidad Nacional del Comahue, Buenos Aires 1400, (8300) Neuquén Capital, Pcia. de Neuquén, Argentina, and CONICET, Argentina

ARTICLE INFO

Article history:
Received 26 August 2011
Received in revised form
17 December 2011
Accepted 31 January 2012
Available online 2 March 2012

Keywords:
XANES
TPR
Reduction-reoxidation
$Ce_{0.9}Zr_{0.1}O_2$

ABSTRACT

The aim of this paper is to gain further insight in the reduction and reoxidation processes taking place when $Ce_{0.9}Zr_{0.1}O_2$ mixed oxides are in reducing or oxidizing atmospheres, respectively. The reduction process of these mixed oxides synthesized by two stoichiometric nitrate-aminoacid gel-combustion routes using glycine and lysine as fuels is studied by conventional H_2-Temperature Programmed Reduction experiments. The results are compared with those obtained by time-resolved *in situ* X-ray absorption near-edge spectroscopy (XANES) in the energy level corresponding to the Ce L_{III} absorption edge. The reoxidation process by this last technique is also studied. Even though the identical composition and crystal structure of both samples, the redox processes resulted very different for each solid, suggesting the influence of specific surface area, pore volume and particle size on them.

1. Introduction

CeO_2–ZrO_2 mixed oxides have been widely studied as catalysts for total oxidation of hydrocarbons, mainly methane [1–3]. These ceria-based catalysts follow the Mars Van Krevelen mechanism, in which the solid delivers its oxygen to oxidize the molecule with the concomitant reduction of its cerium cations. Subsequently, the catalyst is re-oxidized by the incorporation of oxygen molecules present in the surrounding gas-phase, recovering its activity. The complete process is related to the gas–solid interactions taking place on the catalyst surface and the mobility of oxygen vacancies and oxygen anions inside the solid structure. Therefore, the physical and chemical structure of the catalyst surface, the crystal structure and crystallite size would have a strong influence in the whole redox process.

The complete reduction process is quite complex. Many steps should be taken into account, like hydrogen adsorption, hydroxyl formation at the surface, water molecule formation with the concomitant anion vacancy creation and the reduction of two cerium surface cations, water desorption, diffusion of the anion vacancy inside de structure with the further reduction of bulk cerium cations, etc. The whole process will be controlled by the rate-limiting step. Thus, differences in the

* *Corresponding author*. Tel.: +54 1147098158; fax: +54 1147098228.
E-mail addresses: mzimicz@citedef.gob.ar, geno.zimicz@gmail.com (M.G. Zimicz).

0360-3199/$ – see front matter
doi:10.1016/j.ijhydene.2012.01.162

reduction process could be expected for solids with different surface area, pore volume, crystallite size, etc. The redox behavior of these CeO_2–ZrO_2 mixed oxides has been studied mainly by pulse techniques and hydrogen temperature programmed reduction (H_2-TPR) [4–6]. However, further investigations of the redox behavior of these mixed oxides are important in order to get a better understanding of the relation among catalytic activity, redox behavior, structural and morphological properties. In this type of studies, *in situ* analysis techniques have a major role. In particular, the X-ray absorption near the Ce L_{III}-edge spectroscopy (XANES) technique is sensitive to the Ce(IV)/Ce(III) ratio, and therefore, appropriate to follow the reduction and reoxidation processes in ceria-based mixed oxides.

The aim of this work is to gain further insight in the reduction and reoxidation process taking place when $Ce_{0.9}Zr_{0.1}O_2$ mixed oxides are in reducing or oxidizing atmospheres, respectively. The reduction process of $Ce_{0.9}Zr_{0.1}O_2$ mixed oxides synthesized by two stoichiometric nitrate–aminoacid gel-combustion routes using glycine and lysine as fuels is studied by conventional H_2-TPR. The results are compared with those obtained by time-resolved *in situ* XANES spectroscopy in the energy level corresponding to the Ce L_{III} absorption edge. The reoxidation process by this last technique is also studied.

2. Experimental

2.1. Synthesis of mixed oxides

$Ce_{0.9}Zr_{0.1}O_2$ mixed oxides were synthesized by nitrate-aminoacid stoichiometric gel-combustion routes using two different α-aminoacids as fuels, glycine and lysine. The complete description of the synthesis process could be found elsewhere [7]. The solids synthesized using glycine and lysine as fuels will be referred hereafter as sample GS and sample LS, respectively.

2.2. Characterization

Textural characteristics of samples GS and LS were determined by N_2 physisorption at N_2 normal boiling point (−196 °C). Physisorption tests were carried out in a Micromeritics ASAP 2020 Accelerated Surface Area Analyzer and porosimeter.

The structure of both samples was studied by powder X-ray diffraction analyses carried out on a Phillips PW3710 diffractometer with CuK_α radiation, graphite monochromator, and operated at 40 kV and 30 mA. The data were collected in the angular region $2\theta = 20$–$100°$ with a step of 0.02° and counting time of 12 s.

Temperature Programmed tests were carried out using a Micromeritics Autochem II 2720. The samples were placed in a quartz reactor and heated with a 10 °C/min ramp in a 50 $cm^3\,min^{-1}$ flow of a mixture of 5 mol% hydrogen in helium balance. The thermocouple was placed inside the reactor, just above the catalyst bed, in order to avoid heat transfer limitations. H_2 consumption was monitored by measuring the change in the thermal conductivity of the reactor exit gas flow with a thermal conductivity detector (TCD).

2.3. In situ XANES experiments

In situ XANES studies were performed for the Ce L_{III}-edge, in which Ce2*p* electrons are excited with photons of energies above 5720 eV. These tests were carried out in the D06A-DXAS beamline of the Brazilian Synchrotron Light Laboratory (LNLS, Campinas, Brazil). It is a dispersive beamline equipped with a Si (111) monochromator and a CCD detector to collect the absorption spectrum. The Ce L_{III}-edge absorption spectra were recorded in transmission mode. The samples were prepared by mixing GS or LS powders with boron nitride, an inert and weak absorbing binder in the energy band of the experiments. The mixture was pressed into self-supporting discs. In a typical sample preparation, 10 mg of catalyst powder was mixed and pressed with about 80 mg of boron nitride. The sample mass was chosen to give a total absorption ratio of about 1.5. The sample was placed in a sample-holder specially designed for this type of *in situ* measurements, which has a thermocouple that tests sample temperature during the experiment. The sample-holder is placed in a quartz reactor that has inlet and outlet gas lines. The inlet line is connected to a gas-mixing station provided with mass flow controllers. In this way it was possible to reproduce the same conditions used in the conventional TPR tests. After collecting the spectra in a reducing atmosphere, the temperature was lowered to room temperature in an inert atmosphere (He 4.0), and then the samples were subject to a reoxidation process in an oxidizing flow consisted of 5mol% O_2 in He balance. During the reoxidation the sample was heated from room temperature up to 800 °C at a heating rate of 10 °C/min.

2.4. Method of analysis of XANES spectra

XANES spectra were fitted, after background subtraction and intensity normalization, using the software WinXAS [8]. In all cases, a linear combination of standard spectra was used as fitting method. $Ce(NO_3)_3$ and the initial spectrum for each sample, were used as Ce(III) and Ce(IV) standards, respectively. Then the evolution of the reduction percentage with the temperature, $\alpha(T)$, could be determined using the following equations

$$I_{\text{sample}} = f_1 I^0_{\text{sample}} + f_2 I_{Ce(NO_3)_3} \quad (1)$$

$$\alpha(T) = [\text{Ce(III)}/(\text{Ce(III)} + \text{Ce(IV)})] \times 100 = [f_2/(f_1 + f_2)] \times 100 \quad (2)$$

where f_1 and f_2 are the weighting factors of the fitting process, I^0_{sample} is the normalized intensity profile at the beginning of the reduction process, and $I_{Ce(NO_3)_3}$ is the XANES normalized intensity profile of $Ce(NO_3)_3$ standard. This method has been used in the literature to analyze XANES spectra [9,10], and in this work it was chosen among others because it reduces the errors in the determination of the Ce(III)/(Ce(IV) + Ce(III)) ratio. While the method of linear combination reported in the literature generally uses standards of Ce(IV) such as samples of CeO_2, Ce_2S_3, etc., in this work we decided to use the initial spectrum of each sample at room temperature as the pattern

of Ce(IV) because the greatest interest lies in comparing the reduction process of the different samples, and not in the absolute value of the Ce(III) contents. However, in order to determine the amount of Ce(III) species present at the beginning of the reduction process, the initial spectra for each sample were also analyzed taking the XANES profile of cerium dioxide (CeO_2) calcined at 1000 °C as a standard of Ce(IV). The CeO_2 was synthesized by the Liquid-mix method. In this method, citric acid is dissolved in distilled water and, after complete dissolution, is added to the aqueous solution of cerium nitrate. Then, an aqueous 2.5v/v% ethylene glycol solution is incorporated for solution polymerization. Finally, the resulting solution is concentrated in a hot plate at 100 °C for 48 h. The result is a sponge constituted of chains of citrate and cerium, which is grounded in a mortar and calcined in air at 1000 °C, to assure the complete conversion to CeO_2.

3. Results and discussion

3.1. Structure and morphology

XRD patterns presented in Fig. 1 showed that GS and LS samples exhibit the cubic fluorite type crystal structure corresponding to the *Fm3m* space group. No secondary phases or indications of compositional inhomogeneities were detected, even in samples calcined at 900 °C during 2 h. In Table 1 the values of crystallite size (*D*) determined from the analysis of XRD pattern using the Scherrer equation, specific surface area (*A*) and total pore volume (*V*) obtained from N_2 physisorption analysis are summarized. The ratio *d*/*D*, where "*d*" is the particle size calculated as $d = 6/(\rho A)$ (ρ is the theoretical density of each material), is an estimative of the degree of agglomeration of the samples.

As it can be observed from the data presented in Table 1, the aminoacid used in the synthesis produces noticeable modifications in the morphology of the solid obtained. The glycine route yields nanopowders with larger specific surface area and pore volume, and lower degree of agglomeration.

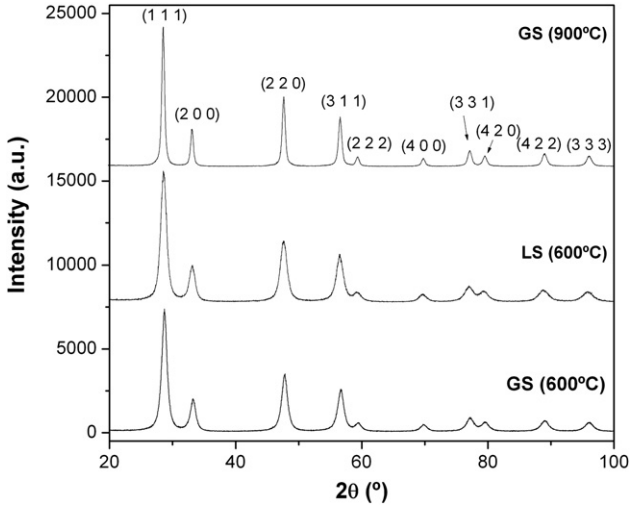

Fig. 1 – XRD patterns for samples GS, LS and sample GS calcined at 900 °C during 2 h.

Table 1 – Structural and morphological properties.

Sample	*D* (nm)	*A* (m^2/g)	*V* (cm^3/g)	*d*/*D*
GS	8.6 (4)	45 (2)	0.086 (4)	2.2 (1)
LS	7.9 (4)	4.9 (3)	0.011 (6)	22 (1)

These differences are probably related to the differences in the aminoacid molecule. Since the glycine molecule is shorter, its combustion is faster and with a higher amount of evolved gases. On the contrary lysine molecule is longer, thus leading to a slower kinetic of combustion and a lower volume of evolved gases. Then, in case of synthesis with lysine the agglomeration of particles and the collapse of the macropores are favored, thereby reducing the BET surface area and total pore volume [7].

3.2. Reduction process

3.2.1. H_2-TPR

In Fig. 2 the TPR profiles for both samples are plotted. Besides, the evolution of the reduction percentage calculated from the H_2 consumption, is depicted as a function of the reduction temperature. From Fig. 2a it is evident that the curves exhibit differences in the position of the peak maxima and in the ratio of peak heights, regardless the fact that both solids have the same composition and crystal structure. Therefore, it is clear that surface area, particle size and pore volume are influencing the reduction process. It is well-known that in the case of oxidation catalysts, such as cerium-based catalysts, which exchange their lattice oxygen ions with the molecule to oxidize, the temperature of the low-temperature peak maximum is a key feature, since it constitutes a kind of measurement of the bond strength of oxygen ions in the crystal structure. Therefore, the position of the low-temperature peak maximum is an indicator of the capability of the solid to release an important quantity of oxygen at a given temperature [11]. It can be seen that the sample GS has a first maximum at 529 °C and sample LS at 621 °C. This would indicate an easy oxygen removal in the area of low temperatures for sample GS. This can also be seen in Fig. 2b, that presents the evolution of the reduction percentage with temperature. Sample GS has reduction percentages higher than sample LS for temperatures up to 630 °C. This is in line with the fact that sample GS has higher surface area due to its minor particle size (nanometric crystallite size and low agglomeration degree). This condition emphasizes the role of the surface in the reduction process. Cerium cations at the surface are less coordinated than bulk ones, thus easing the reduction when they are put in contact with the reducing gas.

Nevertheless, in the temperature range from 630 °C up to 800 °C, sample LS reaches slightly higher reduction percentage values than sample GS. At 800 °C sample GS reaches a 33% of reduction while sample LS 37%. This result is emphasizing the fact that the total reduction process is not only dependent of processes taken place on the surface, like dissociative adsorption of hydrogen, formation of oxygen vacancies at the surface with the corresponding reduction of surface cerium cations, and water desorption, all favored by higher surface areas, but also by other processes like oxygen

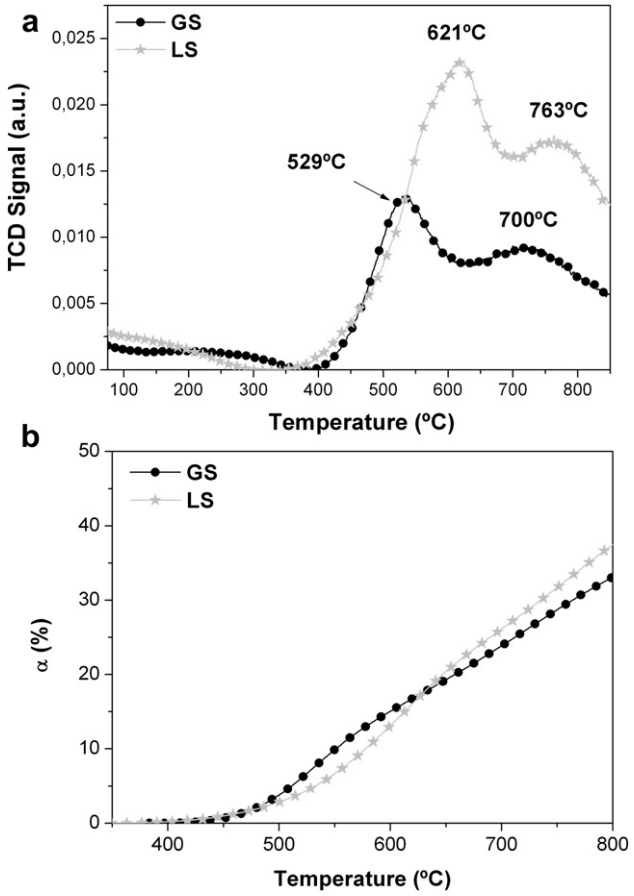

Fig. 2 – (a) Temperature programmed profile. (b) Evolution of reduction percentage with temperature during TPR experiments.

vacancies bulk diffusion with the corresponding reduction of cerium cations in the bulk. This diffusion of vacancies needs to accommodate the vacancies inside the structure and as a consequence would be sensitive to the crystal structure and particle size. In this way, the results are indicating that the higher surface area allows an easy removal of oxygen in sample GS (higher reduction percentage up to 630 °C) but afterwards, another process became important to reach deeper reduction levels.

3.2.2. *Time-resolved in situ XANES*

In Fig. 3 XANES spectra of the standards $Ce(NO_3)_3$ and CeO_2 are presented. The spectra of $Ce(NO_3)_3$ (the Ce(III) standard) has a single absorption maxima at 5726 keV, due to the electronic transition $2p_{3/2} \rightarrow (4f^1)5d$. Hereafter, we will refer it as "A". The spectra of CeO_2 (the Ce(IV) standard) has two peaks located at 5729 keV, referred as "B", and 5737 keV, named "C", which correspond to the $2p_{3/2} \rightarrow (4fL)5d$ and $2p_{3/2} \rightarrow (4f^0)5d$ transitions, respectively. The "L" denotes that an electron in $2p$ orbital of oxygen is transferred to $4f$ orbital of Ce atom [12–15]. The energy difference between "A" and "B" contributions are approximately ~3 eV, in good agreement with data reported in the literature [16]. At room temperature, the spectra of fresh samples exhibit two pronounced absorption maxima, at

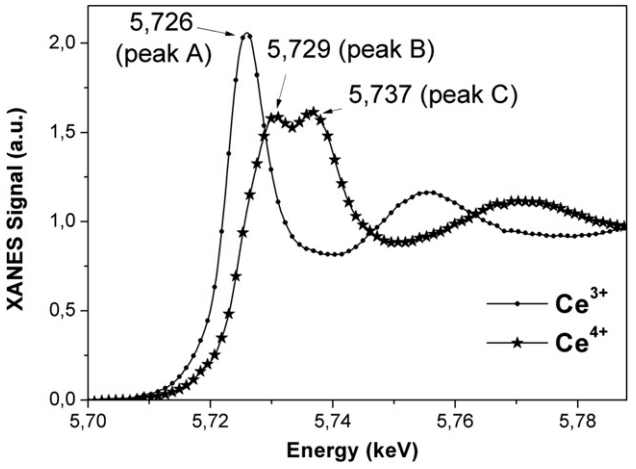

Fig. 3 – XANES spectra in air at room temperature for Ce(III) and Ce(IV) standards.

5729 keV and 5737 keV, respectively, which are in accordance with the observations made for sample CeO_2. Besides, a weak contribution in the region of 5719 keV (pre-edge region), is also observed. This contribution is normally observed in rare earth systems and attributed to a $2p–4f$ quadrupolar transition [12].

In Fig. 4 it is possible to observe the transformation suffered in XANES spectra during the reduction process for both

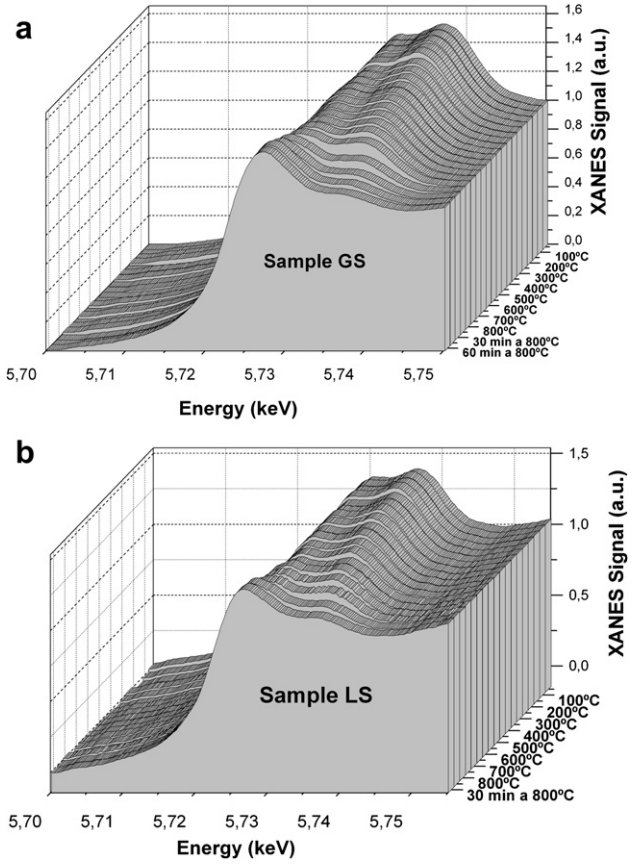

Fig. 4 – Evolution of XANES spectra during the reduction process: (a) sample GS; (b) sample LS.

samples, GS and LS, as a function of temperature. As the temperature increases, and the sample begins to undergo reduction, the peak "C" begins to decrease in intensity, while the opposite occurs with peak "A". This is an evidence of the reduction of Ce(IV) cation to Ce(III). XANES spectra acquisition under reduction conditions was made in two identical experiments for each sample, over discs of similar characteristics, obtaining an excellent reproducibility of the results. At low temperatures, the error was very low, but it increased with increasing temperature, reaching a maximum of ±3% at 800 °C. These values are comparable to errors reported in the literature for other methods [12,16,17]. The initial spectra of each sample were processed with the same fitting procedure, and the Ce(III) content in the fresh samples was obtained. These values are 0.6 (±0.5) and 1.0 (±0.7)% for samples GS and LS respectively, indicating that the fresh solids are almost completely oxidized. By applying the fitting procedure described in the methodology item we obtained the evolution of the reduction percentage with temperature. These results are shown in Fig. 5, superimposed with the same percentage obtained from the TPR experiments. The start of the reduction process was detected at significantly lower temperatures, approximately at 200 °C using XANES results, while by TPR no significant reduction was observed at temperatures above 400 °C. However, a good agreement between both techniques was observed, obtaining very similar final percentages of reduction at 800 °C. By XANES studies, sample GS reached a 34% of reduction, while the sample LS suffered a reduction of 39%.

3.3. *Reoxidation process*

After reaching 800 °C during the reduction process, the temperature and atmosphere conditions were maintained for 30 min, to assess the maximum level of reduction. The degree of reduction reached is similar in both cases, and close to 55%. In Fig. 6 the *in situ* XANES results for the reduction and reoxidation processes are plotted superimposed.

After the reduction process was considered finished, the samples were cooled to room temperature in an atmosphere of He 4.0 (5 ppm of oxygen as an impurity). The level of reduction varies greatly when the starting point for the reoxidation process is compared with the endpoint of the reduction process. Samples LS and GS ends the reduction process with a percentage close to 55%, but begin the cycle of oxidation with 35% and 25% respectively. This marked drop in the degree of reduction is due to the reoxidation of the Ce(III) species formed previously, with oxygen impurities present in

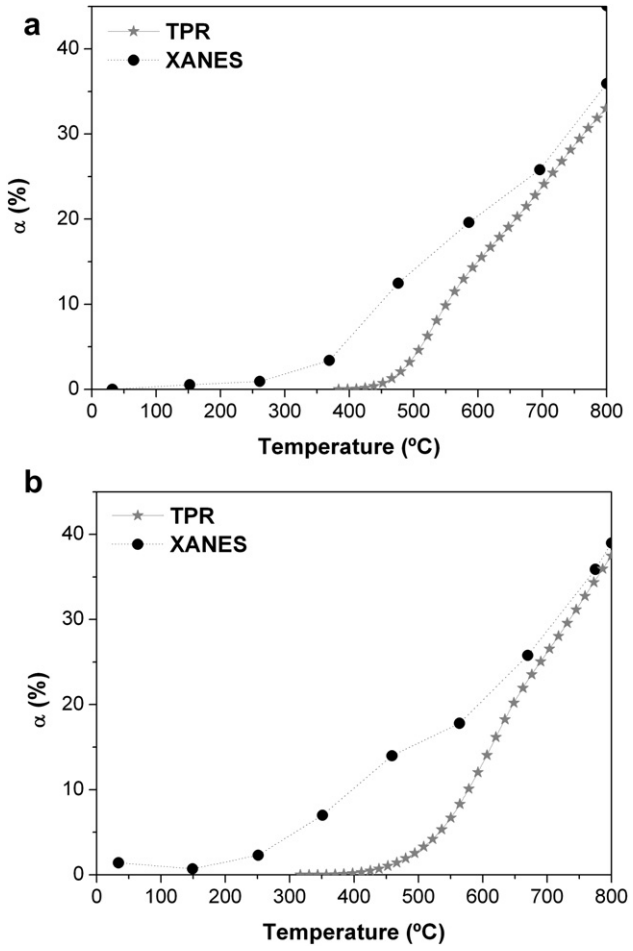

Fig. 5 – Comparison of the evolution of $\alpha(T)$ observed in TPR and in situ XANES reduction experiments for: (a) sample GS, (b) sample LS.

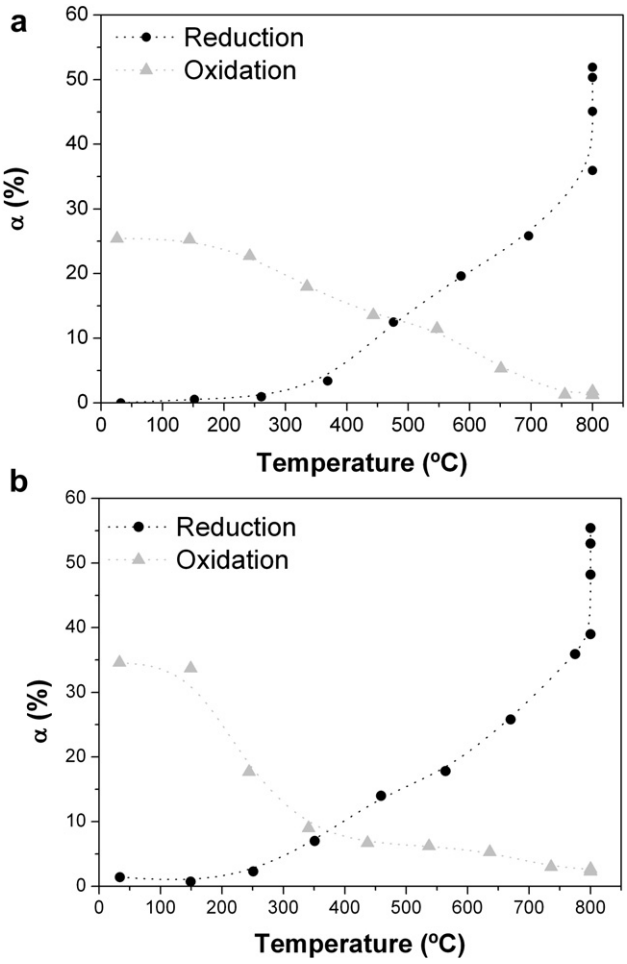

Fig. 6 – *In situ* XANES study of the evolution $\alpha(T)$ during reduction and reoxidation treatments: (a) sample GS, (b) sample LS.

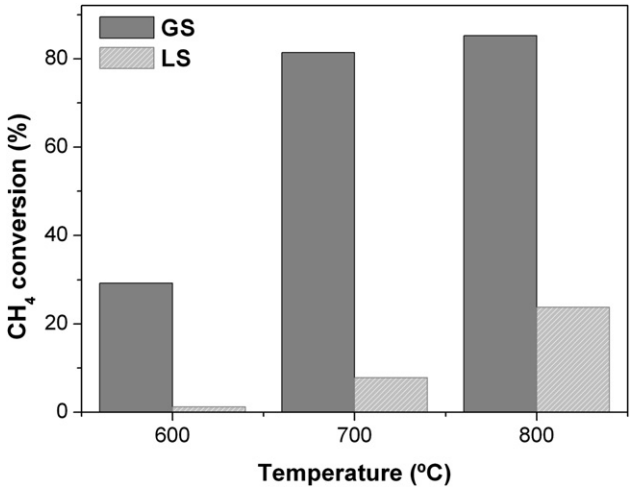

Fig. 7 – CH_4 conversion for samples GS and LS, in the same operating conditions, with feed composition corresponding to total oxidation reaction.

He. This fast reoxidation of cerium species by exposure to even small amounts of O_2 was previously observed by other researchers [11]. It should be noted that the sample GS is more easily oxidized in the presence of only 5 ppm of O_2.

Fig. 6b shows that the sample LS is re-oxidized slowly below 150 °C, very fast at temperatures in the range 150–300 °C and then the reoxidation rate is drastically reduced, so that in the temperature range between 300 °C and 800 °C the degree of reduction change from about 10% to 2%, approximately. In contrast, sample GS shows a reoxidation rate nearly constant in the range of temperatures between 150 °C and 750 °C. These results indicate big differences in the reoxidation process for both samples, despite being two solids with the same composition and crystal structure. It is no easy to speculate what is the governing rate-limiting step, even though the fact that samples suffered reoxidation during their return to room temperature and only with the scarce quantity of oxygen present in Helium. Further investigations should be necessary in order to adjust different models considering different rate-limiting processes. Nevertheless, it is important to observe that both samples completely recover the oxygen inside the structure, a very important feature for an oxidation catalyst.

Finally, it is worth to mention that these samples showed very different catalytic behavior. In Fig. 7 methane conversion in total oxidation conditions, at three different temperatures are presented. It is possible to say that, up to 700 °C, sample GS showed higher values of methane conversion than sample LS, being in particular at 700 °C 80% and 10% respectively. This great difference could not be explained only with the difference in specific surface area and indeed the different redox behavior observed should have influence on it [6].

4. Conclusions

The time-resolved *in situ* XANES technique appears as a very powerful tool to study the redox behavior of catalysts. These tests exhibited very good reproducibility and provided important information related to the reduction and reoxidation processes of the solids. It was determined that the different gel-combustion synthesis routes yield materials with different morphological properties, and this leads to different kinetics of reduction and reoxidation.

The onset of the reduction of Ce(IV) cations was identified at lower temperature by XANES technique than that observed by TPR. However, the reduction achieved at the end of the experiments was very similar for both techniques. On the other hand, even though the identical composition and crystal structure, the redox processes resulted very different for each sample, suggesting the influence of specific surface area, pore volume and particle size on them.

Acknowledgements

This work was supported by the Brazilian Synchrotron Light Laboratory (LNLS) under proposals D06A-DXAS-9949, Agencia Nacional de Promoción Científica y Tecnológica (Argentina, PAE-PICT 2007 No. 2288 and PICT 2007 No. 1152), CNPq (Brazil, PROSUL Program, Project # 490580/2008-4) and CLAF.

REFERENCES

[1] Pengpanich S, Meeyoo V, Rirksomboon T, Bunyakiat K. Appl Catal., A 2002;234:221–33.
[2] Bozo C, Guilhaume N, Garbowski E, Primet M. Catal Today 2000;59:33–45.
[3] Larrondo S, Vidal MA, Irigoyen B, Craievich A, Lamas DG, Fábregas IO, et al. Catal Today 2005;107-108:53–9.
[4] Kaspar J, Fornasiero P, Graziani M. Catal Today 1999;50: 285–98.
[5] Fornasiero P, Di Monte R, Ranga Rao G, Kaspar J, Meriani S, Trovarelli A, et al. J Catal 1995;151:168–77.
[6] Zimicz MG, Lamas DG, Larrondo SA. Catal Commun 2011;15: 68–73.
[7] Zimicz MG, Fábregas IO, Lamas DG, Larrondo SA. Mater Res Bull 2011;46(6):850.
[8] Ressler T. J Synchrotron Radiat 1998;5:118.
[9] Skinner SJ, Packer RJ, Bayliss RD, Illy B, Prestipino C, Ryan MP. Solid State Ionics 2011;192:659–63.
[10] Jacobs G, Davis BH. Int J Hydrogen Energy 2010;35: 3522–36.
[11] Conesa JC, Fernández-García M, Martínez-Arias A. In: Trovarelli A, editor. Catalysis by ceria and related materials. London, UK: Imperial College; 2001. p. 169–216. Chapter 5.
[12] Soldatov AV, Ivanchenko TS. Phys Rev B Condens 1994;50(8): 5074–80.
[13] Kaindl G, Schmiester G, Sampathkumaran EV, Wachter P. Phys Rev B 1988;38:10,174–10,177.
[14] Bianconi A, Marcelli A, Dexpert H, Karnatak R, Kotani A, Jo T, et al. Phys Rev B 1987;35:806–12.
[15] Takahashi Y, Sakami H, Nomura M. Anal Chim Acta 2002; 468:345–54.
[16] El Fallah J, Boujana S, Dexpert H, Kiennemann A, Majerus J, Touret O, et al. J Phys Chem 1994;98:5522–33.
[17] Assefa Z, Haire RG, Caulder DL, Shuh DK. Spectrochim Acta, Part A 2004;60:1873–81.